BIBLIOGRAPHIC INFORMATION SYSTEM

Journal Full Title: Journal of Biomedical Research & Environmental Sciences
Journal NLM Abbreviation: J Biomed Res Environ Sci
Journal Website Link: https://www.jelsciences.com
Journal ISSN: 2766-2276
Category: Multidisciplinary
Subject Areas: Medicine Group, Biology Group, General, Environmental Sciences
Topics Summation: 130
Issue Regularity: Monthly
Review Process: Double Blind
Time to Publication: 21 Days
Indexing catalog: Visit here
Publication fee catalog: Visit here

DOI: 10.37871 (CrossRef)
Plagiarism detection software: iThenticate
Managing entity: USA
Language: English
Research work collecting capability: Worldwide
Organized by: SciRes Literature LLC

IndexCopernicus ICV 2020: 53.77

Manuscript should be submitted in Word Document (.doc or .docx) through

Online Submission

form or can be mailed to support@jelsciences.com

Vision: Journal of Biomedical Research & Environmental Sciences main aim is to enhance the importance of science and technology to the scientific community and also to provide an equal opportunity to seek and share ideas to all our researchers and scientists without any barriers to develop their career and helping in their development of discovering the world.

JOURNAL OF BIOMEDICAL RESEARCH & ENVIRONMENTAL SCIENCES
issn: 2766-2276
SUBJECT AREA(S): IMMUNOLOGY
DOI: 10.37871

RESEARCH ARTICLE

A New CpG ODN Induces a Fine-Tuning of Innate Response Resulting in *Mycobacterium tuberculosis* Containment

Giulia Cappelli[1], Daniela Giovannini[2,5#], Annalisa Basso[3], Annalucia Serafino[2], Federica Andreola[2], Vittorio Colizzi[4] and Francesca Mariani[1]*

[1]Institute for Biological Systems, National Research Council Via Salaria km 29,300, 00015, Montelibretti (RM), Italy
[2]Institute Translational Pharmacology, National Research Council, Via Fosso del Cavaliere, 00133, Rome, Italy
[3]Institute of Biochemistry and Cellular biology, National Research Council, Via E. Ramarini, 32, 00016, Monterotondo Scalo (RM), Italy
[4]Department of Biology, University of Rome "Tor Vergata", Via della Ricerca Scientifica, 00133, Rome, Italy
[5]ENEA, Laboratory of Biomedical Technologies, Casaccia Research Center, 00123 Rome, Italy
[#]The authors equally contributed to the study

ABSTRACT

Synthetic oligodeoxynucleotides containing bacterial CpG motifs trigger an immunomodulatory response that correlates with both the CpG hhhexamers and their flanking regions. In this study, four new phosphodiester backbone CpG ODNs were studied in the contest of the innate immune response to *Mycobacterium tuberculosis* (MTB) infection. Two out of the four CpG ODNs (CpG2 and CpG3) displayed significant and opposite immunomodulatory effects: CpG2 enhanced MTB containment by human Monocyte-Derived-Macrophages (MDM), while CpG3 promoted an increased pathogen growth, higher ROS and Labile Iron Pool (LIP) levels. Accordingly, for iron homeostasis genes transcription, CpG2 and CpG3 induced, respectively, an iron retention and iron release phenotype.

Moreover, CpG2 induced NLRC4 and TRAF6 gene expression and repressed IKK alpha and TREM1 while CpG3 induced PPBP and IL-36 RN and repressed TRAF6, IL-1B, IL-1R2 and NF-kB2. After MTB infection, CpG2 increased the release of soluble TREM1 protein among many others as compared with fewer innate response-associated proteins induced by CpG3. We suggest that CpG2 helps the containment of MTB infection, by inducing an early tight balance of MDM activation players, including LIP, chemokines, ROS and TREM1 receptors. Oppositely, CpG3 induces in MDM an excessive and unregulated inflammatory response unable to contain MTB infection.

Abbreviations

MDM: Human Monocyte-Derived-Macrophages; ROS: Reactive Oxygen Species; ipH: Intracellular pH; LIP: Labile Iron Pool; MTB: *Mycobacterium tuberculosis H37Rv* strain; CFU: Colony Forming Units; CpG motif: Unmethylated Cytosine-Guanine di-nucleotide, located in a given hhexamer; CpG ODN: Synthetic Oligodeoxynucleotide Containing a CpG Motif; PAMP: Pathogen Associated Molecular Pattern; DAMP: Danger Associated Molecular Pattern; PRRs: Pathogen Recognition Receptors; TLR: Toll-like Receptor; TREM1: triggering receptor expressed on myeloid cells1; s-TREM1: soluble TREM1; Tf: Transferrin; TfR1: Transferrin receptor 1; FerrH: Ferritin Heavy chain; Fp: Ferroportin (or SLC40A1); Nramp1: Natural Resistance-Associated Macrophage Protein 1 (or SLC11A1) ; HOX1: Heme-Oxygenase1.

***Corresponding author**

Francesca Mariani, Institute for Biological Systems, National Research Council, c/o Area della Ricerca di Roma1 – Montelibretti (RM), Via Salaria Km 29,300, Italy

E-mail: francesca.mariani@cnr.it

DOI: 10.37871/jbres1517

Submitted: 27 July 2022

Accepted: 30 July 2022

Published: 30 July 2022

MEDICINE GROUP

IMMUNOLOGY

VOLUME: 3 ISSUE: 7 - JULY, 2022

How to cite this article: Cappelli G, Giovannini D, Basso A, Serafino A, Andreola F, Colizzi V, Mariani F. A New CpG ODN Induces a Fine-Tuning of Innate Response Resulting in *Mycobacterium tuberculosis* Containment. J Biomed Res Environ Sci. 2022 July 30; 3(7): 802-818. doi: 10.37871/jbres1517, Article ID: JBRES1517, Available at: https://www.jelsciences.com/articles/jbres1517.pdf

Introduction

Unmethylated-Cytosine-Guanine dinucleotide (CpG) motifs are potent stimulators of the host immune response. During the last decade, CpG have been studied for their application in therapeutic and vaccine strategies, while are still limited the studies elucidating their stimulating role in the innate response to bacterial infections. These bacterial sequences are considered a type of Pathogen-Associated Molecular Pattern (PAMP) due to their abundance in bacterial genomes, and their immunostimulatory capacity against many intracellular pathogens, including *Listeria monocytogenes, Leishmania major*, *Francisella tularensis, Klebsiella pneumonia* [1-6] *Staphylococcus aureus* [7] and *Mycobacterium tuberculosis* (MTB) [8,9-11] have been documented. Some studies were performed, primarily, to describe their adjuvant properties in mice, but few data are available on the effects of CpGs in humans. It has been shown that mice vaccinated with BCG plus CpG Oligodeoxynucleotide (ODN) had a greater reduction in bacterial loads, after infection with MTB, than those vaccinated with BCG alone [12].

Juffermans, et al. [13] found that mice infected with virulent MTB are protected by CpG ODN and that this effect is abrogated in IFN-γ gene-deficient mice. Structurally, the synthetic unmethylated CpG dinucleotide are mainly designed between 2 purines at 5' and 2 pyrimidines at the 3' end, which can improve their immune effects when flanked by specific sequences constituted by TC di-nucleotide at the 5' end and CTC tri-nucleotide pyrimidine at the 3' end.

Moreover, most synthetic CpG ODNs differ from microbial DNA because they have a partially or completely modified Phosphorothioate (PTO), instead of the phosphodiester, backbone, to protects the ODN from the attack of cellular nucleases. In the last years several clinical studies showed that PTO modification may induce undesired effects such as reduced protective immune responses, lymphoadenopathy, sustained local interferon gamma and IL-12 production, prolongation of coagulation time, complement activation, acute toxicity and renal damage [14]. To circumvent these side effects the research, recently, focused on several CpG ODNs with an unmodified phosphodiester backbone and a number of studies have been performed to investigate the effects of DNA sequence as well as DNA backbone modification on cellular uptake and immune stimulation.

A recent study report that the TLR9 binding site exhibits a strong bias in favor of a phosphodiester backbone over the phosphorothioate backbone of the CpG motif, suggesting the role of unmodified backbone to design improved immunostimulatory TLR9 agonists [15,16]. It is known that CpG-ODN, as well as bacterial DNA, can directly stimulates macrophages, and their uptake occurs through endocytosis followed by endosomal maturation, characterized by the passage of the endosomes in the lysosomes compartments. The endosomes fusion and the vesicles trafficking are regulated by the intracellular pH (ipH): in fact, some compounds, able to interfere with the intracellular acidification, may affect the endosomal fusion and the biological action of CpG ODN [17]. It was also documented that the acidification of endosomes containing CpG DNA is coupled with the rapid generation of ROS that, if produced in excess, are generally considered to be cytotoxic and have been implicated in pathogenesis in a wide variety of diseases. As opposite, moderate concentrations of intracellular ROS influence gene expression, at the level of transcriptional factors as Nuclear Factor κB (NF-κB) and Activator Protein 1 (AP-1) [18]. Some authors reported that the responses of both B cells and monocyte-like cell lines to DNA containing CpG motifs were sensitive to endosomal acidification for the production of the cytokines IL-6, IL-12 and TNF-α [19]. It has been described [20] that the production of ROS can be highly increased by the presence of intracellular Labile Iron Pools (LIP) that is the chelatable, ferrous and redox-active iron. Therefore, iron metabolism needs to be tightly controlled in mammalian cells by iron-binding proteins, such as Transferrin and Ferritin [21] to avoid an uncontrolled Fenton's reaction favoured by the presence of ROS. In brief, Transferrin Receptor 1 (TfR19 mediates the entry in the cell of Transferrin-bound iron, while Ferritin (FERR Heavy and Light chain) has the function to store iron in cell organelles, while, in contrast, Ferroportin (Fp) allows iron to exit in the extracellular space. Nramp1 is a divalent cation transporter located on the lysosomal membrane, and it is described to be able to either concentrate iron in the lysosome, or, conversely, to deprive the intra-phagolysosomal pathogen of the precious metal. Heme Oxygenase 1 (HOX1) degrades Heme, produces Carbon Monoxide (CO), bilirubin and free ferrous iron, and it is also known to exert an anti-oxidant and a cytoprotective role in the cells. In this respect, it has been shown that the cellular activation state controls the homeostasis of iron in human macrophages [22,23].

Innate immunity is critical for host survival during the early stages of infection. Both bacterial DNA and CpG ODN could induce cytokines production such as TNF-α, IL-12 and IL-6. However, fine-tuning of this response is critical to prevent excessive inflammation and tissue damage. The CpG ODN-induced activation of the innate immune cells, leading to clear the pathogen and to shape the adaptive immune response, is triggered by the recognition and internalization of CpG with different receptors, such as the toll-like receptors (as TLR9).

Furthermore CpG-ODN-induced TLR9 activation, either alone or in combination with LPS, resulted in a significant increase of supernatant sTREM-1, the soluble form of triggering receptor [24] expressed on myeloid cells (TREM1). This latter, in the membrane anchored form, can modulate the innate response either by amplifying or dampening TLR-induced signals, and thus play critical roles in fine-tuning the inflammatory response.

In this scenario, we investigated the role of new phosphodiester CpG-ODN in influencing human macrophages activation linked to their mycobactericidal capacity. We confirmed that the CpG flanking sequences play a specific role in regulating the antibacterial response [25]. According to the most effective and opposite properties induced by two out of the four new CpG-ODNs (CpG2 and CpG3) in influencing MDM bacterial containment we further studied several parameters related to the activated innate immune response.

We contemporarily analysed CpG-ODN effects on ipH, ROS release and LIP. To better understand the inflammation status and regulation induced by the two CpG ODNs we investigated the variations in cytokines/chemokines and iron homeostasis genes expression before and after MTB infection. We focused our attention on a group of iron regulating genes mainly involved in the macrophage response to infection, such as TfR1, Ferr H, HOX1, Fp and Nramp1. Finally, we measured the innate response associated proteins released in CpG-treated MDM supernatants.

The traits associated to MTB containment or permissiveness are presented and the possible role in conferring protective immunity of an early, acute, but timely self-limited inflammatory innate immune response [26] is discussed.

Materials and Methods

CpG motifs and ODNs sequences

In tables 1A,B are reported the sequences of our four phosphodiester backbone CpG motifs, and our four reverse CpG (Table 1A) and their flanking sequences. They contain a 5' TCG and a 3' CTC (in italic) in order to improve their immune effects (10-11). In each CpG-rev the CpG motif (hexamer) is left intact but loses the right flanking sequence context, which is the reverse complement of initial flanking sequences.

Current evidence suggests that TLR9 show considerable selectivity for CpG DNA sequences with different preferences in mouse (GACGTT) and human (GTCGTT) species. Given that our new CpG2 ODN contains the hexamer used in mouse studies, we included also a human motif ODN, containing the human hexamer, to verify whether they elicit a species-restricted response.

Sample size

Buffy coats from 10 different healthy donors have been collected to perform the experiments and each donor have been analysed only once. The number of donors tested in each specific measurement is indicated in the figure legends.

Cell culture and treatment

Monocytes were isolated from 10 healthy donors' buffy coats Peripheral Blood Mononuclear Cells (PBMC) by density gradient centrifugation using Lympholyte-H (Cederlane, Mayada). Cells were grown in complete medium consisting of RPMI 1640 supplemented with 10% FBS, 2 mM L-glutamine and gentamicin 5 μg/ml at 37°C in a 5% CO_2 atmosphere. The day after the Monocyte-Derived-Macrophages (MDM) differentiated by adherence, were detached and resuspended 10^6/ml. At the seventh day 10^6 differentiated monolayer cells, were stimulated for 1 hr with 1 μM of different CpG ODNs (Table 1) and GpC ODN (*ATCG*ACTCTCG**GAGCTT***CTC*) [27].

Intracellular pH measurement

Intracellular pH (ipH) was measured using the intracellular probe 2"-7"-bis (carboxyethil)-5(6)-carboxyfluorescein (BCECF/AM) according to the protocol described by Grinstein, et al. [28].

MDM were treated with CpG ODN 1, 2, 3 and 4 and tested in parallel in a 30-minute time interval of repeated measures. The ipH was measured with a BCECF/AM intracellular probe (which is proportional to ipH values). Both untreated than GpC treated macrophages were used as negative control. Briefly, $2x10^6$ of uninfected macrophages were treated with different CpG ODNs (as described above), washed and incubated with 1μg/ml of BCECF/AM, dissolved in DMSO, at 37°C for 30 minutes, and protected from the light. The role

Table 1a: Sequences of the four CpG ODN employed, and the relative reverse complementary flanking sequences for each CpG ODN, referred to as CpG-rev. The CpG motifs, with two Purines 5' and two Pyrimidines 3', are in bold, the CpG dinucleotides are underlined, and the 5' TCG and 3' CTC sequences are in italic. In each CpG-rev the CpG motif is left intact but loses the appropriate flanking sequence.

CpG1	*ATCG*ACTCTCG**GACGTC***CTC*
CpG1rev	GAG**GACGTC**CGAGAGTCGAT
CpG2	*ATCG*ACTCTCG**GACGTT***CTC*
CpG2rev	GAG**GACGTT**CGAGAGTCGAT
CpG3	*ATCG*ACTCTCG**AACGTC***CTC*
CpG3rev	GAG**AACGTC**CGAGAGTCGAT
CpG4	*ATCG*ACTCTCG**AACGTT***CTC*
CpG4rev	GAG**AACGTT**CGAGAGTCGAT

Table 1b: Sequences of the commercial CpG used are reported, the CpG dinucleotides are underlined.

CpG human	ATCGACTCT**CG**GTCGTTCTC
2006	TCGTCGTTTTGT**CG**TTTTGTCGTT
1668	TCCATGA**CG**TTCCTGATGCT

Table 1c: Rationale for the design of our four new CpG-ODNs. We started with the well-known CpG motif, described by Krieg in 2002 [27] there after called CpG2 ODN with the newly designed flanking sequences. Then we asked whether it might have conserved its effects when the hhexamer was the reverse-complement (thereafter called CpG3). CpG1 and CpG4 are the result of the variation of the final Pyrimidine in, respectively, CpG2 and CpG3.

	5′		CpG dimer		3′			
	Pur.	Pur.	C	G	Pyr.	Pyr.		
CpG1	G	A	C	G	T	C	Variation of final Pyrimidin CpG2	Our design
CpG2	G	A	C	G	T	T	Optimal CpG motif	Krieg 2002
CpG3	A	A	C	G	T	C	Rev. Complem. CpG2 motif	Our design
CpG4	G	A	C	G	T	T	Variation of final Pyrimidin CpG3	Our design

of the Na^+/H^+ exchanger was detected in the Hepes buffer without bicarbonate with the following composition: 140 mM NaCl, 5 mM KCl, 1 mM $CaCl_2$, 1 mM $MgCl_2$, 20 mM Hepes, 10 mM glucose at pH = 7.4. Fluorescence was measured under continuous magnetic stirring at the controlled temperature (37˚C) in a Perkin-Elmer L-S-5 luminescence spectrometer equipped with a chart recorder model R 100A, with excitation and emission wavelengths, respectively, of 500 and 530 nm using 5 and 10 nm slits. The ipH variations are indicated with Fluorescence Arbitrary Units (F.A.U.).

One-Way ANOVA (Bonferroni post-test) was used for the statistical analysis.

The fluorescent probe used detected the overall ipH. Although we could not discriminate between cytosolic and organelles pH values, a statistically relevant ipH modification was observed in treated versus untreated cells.

Arbitrary fluorescence units were normalised on the untreated MDM maximum value and the trend of intracellular acidification was plotted.

Infection of MDM with MTB H37Rv or *S.aureus*

The infection was performed after seven days of MDM culture, at a Multiplicity of Infection (MOI) of 10:1 (bacteria to cells), following 1 hour of pre-treatment with 1 µM of CpG ODNs. As control cells, MDM only infected but not CpG treated, were used. The experiments were repeated on MDM samples from 10 healthy donors. Prior to infection, MTB bacilli were sonicated to disrupt small aggregates (clumps) of bacteria. In respect with *S.aureus* infection the sonication step was not necessary.

Determination of bacterial Colony Forming Units (CFU)

Infection with *S.aureus:* MDM were treated with CpG ODNs for 1 hour, and then infected with *S.aureus* at a MOI of 10. After 3 hours of infection, the cells were washed with warm Phosphate Buffer Saline (PBS), to eliminate all the non-phagocytosed bacteria, and left for 24 hours to measure the intracellular bacterial replication by CFU measure. Part of the cells was immediately lysed (0.1% Saponin -Sigma, St Louis, MO- PBS for 30 minutes at 37°C) to calculate the phagocytosis rate. The remaining infected MDM were left in culture for 24 h, and then the culture supernatant was harvested and the cells lysed, according to specific protocols, to determine the intracellular bacterial growth and to extract the corresponding total RNA. CFU determination for MTB and *S.aureus*.

Cell lysates were serially diluted and plated on 7H10 Middlebrook (Becton Dickinson, Franklin Lakes, NJ, USA) medium with OADC in duplicate, for *M.tuberculosis* or Mueller-Hinton Agar plates for *S.aureus*. CFU were counted after 21 days (for slow growing *M.tuberculosis*) or 24 h (for fast growing *S.aureus*) of incubation at 37˚C in a 5% CO_2 atmosphere and plates were maintained for 30 days to ensure that no additional CFU appeared. *S.aureus* phagocytosis rate was measured after two hours of infection: the cells have been washed twice to eliminate the extracellular bacteria and subsequently the cell lysates have been plated and incubated for 24 hours.

The rate of phagocytosed bacteria was calculated by dividing the CFU obtained from intracellular bacteria entered in two hours of infection by the total number of bacteria used to infect MDMs. This rate was calculated only for *S.aureus* infection, given its fast growing cell cycle (20 min), as compared with the slow growing MTB one (16 hr). In order to accurately determine the effective Multiplicity of Infection (MOI) and to eliminate the errors due to the possible variation of the independent experiments, the bacterial stocks titers used was confirmed each time (by plating the final dilution used to infect the cells).

Cells treatment: In the experiments with the CYBB (or gp91 phox) inhibitor Diphenyleneiodonium Chloride (DPI), alone or in combination with CpG ODNs, cells were pre-treated for 1 hour and then infected. The final concentration was 10µM DPI which was co-administered with CpG-ODNs.

Reactive oxygen species detection: ROS generation was analysed, as previously described [29] by loading cells with 10 µM of the cell permeant fluorescent indicator 2', 7'-dichlorofluorescein diacetate (H_2DCFDA) (Molecular Probes) for 60 minutes at 37˚C in the dark. Upon cleavage of the acetate groups by intracellular esterases and oxidation, the non-fluorescent H_2DCFDA is converted to the highly fluorescent 2', 7'-dichlorofluorescein (DCF). DCF fluorescence intensity is proportional to the ROS amount produced intracellularly [18]. After labelling, 10^6 MDM cells

Table 2: List of genes and proteins.

Gene or Protein name	Description	Alternative nomenclature
Nramp1	Natural resistance-associated macrophage protein 1	SLC11A1, Solute Carrier Family 11 (Proton-Coupled Divalent Metal Ion Transporters), Member 1
PPBP	Pro-platelet basic protein (chemokine (C-X-C motif) ligand 7)	B-TG1, Beta-TG, CTAP-III, CXCL7
IL-36RN	Interleukin 36 receptor antagonist	IL-1R antagonist
CHUK	Conserved helix-loop-helix ubiquitous kinase	IKBKA, IKK-alpha, IKK1, IKKA, NFKBIKA
CCR3	Chemokine (C-C motif) receptor 3	CC-CKR-3, CD193, CKR3, CMKBR3
TREM1	Triggering receptor expressed on myeloid cells 1, amplifier of inflammatory responses that are triggered by bacterial and fungal infections and is a crucial mediator of septic shock.	CD354 Antigen
IL-1R2	Interleukin 1 receptor, type II	CD121b, IL1RB
NLRC4	NLR family, CARD domain containing 4	
TRAF6	TNF receptor-associated factor 6	MGC:3310, RNF85
CCL1	Chemokine (C-C Motif) Ligand 1, Inflammatory Cytokine I-309, Cytokine that is chemotactic for monocytes but not for neutrophils. Binds to CCR8.	I-309
CCL2	Chemokine (C-C Motif) Ligand 2, Monocyte Chemotactic Protein 1, it binds to chemokine receptors CCR2 and CCR4.	MCP-1
CCL3	Macrophage Inflammatory Protein 1-Alpha, G0/G1 Switch Regulatory Protein 19-1, binds to CCR1, CCR4 and CCR5.	MIP-1 alpha
CCL4	Macrophage Inflammatory Protein 1-Beta, binds CCR5 but it is a ligand also for CCR1 and CCR2	MIP-1 beta
CCL5	Small Inducible Cytokine A5, binds to CCR5	RANTES
CXCL1	Growth-Regulated Alpha Protein, the encoded protein is a secreted growth factor that signals through the G-protein coupled receptor, CXCR2.	GRO-alpha
CXCL10	Interferon-Inducible Cytokine IP-10, binding of this protein to CXCR3 results in pleiotropic effects, including stimulation of monocytes, and modulation of adhesion molecule expression	IP-10
CXCL11	Interferon Gamma-Inducible Protein 9, binds to CXCR3	I-TAC
CXCL12	This antimicrobial gene encodes a Stromal Cell-Derived Factor 1. Activates the C-X-C chemokine receptor CXCR4 to induce a rapid and transient rise in the level of intracellular calcium ions and chemotaxis.	SDF-1
MIF	Macrophage Migration Inhibitory Factor, Pro-inflammatory cytokine. Involved in the innate immune response to bacterial pathogens. The expression of MIF at sites of inflammation suggests a role as mediator in regulating the function of macrophages in host defence. Counteracts the anti-inflammatory activity of glucocorticoids.	GLIF, DER6, MMIF
PAI1	Plasminogen Activator Inhibitor Type 1, is the principal inhibitor of tissue plasminogen activator (tPA) and urokinase (uPA), and hence is an inhibitor of fibrinolysis and ECM degradation.	Serpin E1
IL-8	Monocyte-Derived Neutrophil Chemotactic Factor, binds CXCR1 and CXCR2; it functions as a chemoattractant, and is also a potent angiogenic factor.	CXCL8
G-CSF	Granulocyte Colony Stimulating Factor, Granulocyte/macrophage colony-stimulating factors are cytokines that act in haematopoiesis by controlling the production, differentiation, and function of 2 related white cell populations of the blood, the granulocytes and the monocytes-macrophages.	CSF beta, CSF3
GM-CSF	Granulocyte Macrophage-Colony Stimulating Factor. The protein encoded by this gene is a cytokine that controls the production, differentiation, and function of granulocytes and macrophages. The active form of the protein is found extracellularly as a homodimer. This gene has been localised to a cluster of related genes at chromosome region 5q31, which is known to be associated with interstitial deletions in the 5q- syndrome and acute myelogenous leukaemia.	CSF alpha,CSF2
sTREM1	Soluble TREM1, sTREM-1 is thought to negatively regulate TREM receptor signalling through neutralisation of the ligand.	
CD55	Decay Accelerating Factor for Complement	DAF
IL1RAP	IL-1 Receptor Accessory Protein	
CYBB	Cytochrome B-245 Heavy Chain	gp91 PHOX

List of genes and proteins analysed by real time PCR and protein array (abbreviation, description and alternative nomenclature).

were washed twice with PBS, centrifuged for 10 minutes at 580 g, resuspended in PBS buffer and stimulated with the different CpG ODNs. ROS production was determined at 45 minutes after CpG ODN stimulation by fluorimetric measurement of fluorescence (excitation 488 nm; emission 530 nm). Fluorescence emission was monitored by the use of a Perkin Helmer LS50B Luminescence Spectrometer.

3.6.4.**Quantification of the labile iron pool**: The labile iron pool was measured by loading cells with the iron-sensitive probe Calcein-AM (Molecular Probes) as previously described [30]. Briefly, human MDM were incubated in 12-well plates with αMEM supplemented with 1 mg/mL bovine serum albumin and 0.25 μM Calcein-AM at 37˚C for 15 minutes. After two washing cycles, cells were maintained in HBSS supplemented with 10 mM glucose and fluorescence was measured using the Victor3 Multilabel Counter (Wallac, Perkin Elmer) at 485 nm (excitation) and 535 nm (emission).

The iron chelator Deferiprone (Sigma) was then added to reach 300 μM final concentration and fluorescence was re-determined after 10 minutes. Fluorescence increases induced by iron chelator were normalised on protein content, assessed by the BCA assay, and considered as Labile Iron Pool (LIP) values, calculated by the formula: [CA-Fe] = ΔF * [CAt].

CA is Calcein, Fe is Iron, [CA-Fe] is the concentration of the Iron-bound CA, [CA] t is the total concentration of intracellular CA, and DF is the increase in the fluorescence produced by the addition of the chelator Deferiprone. The concentration of iron-bound CA [CA-Fe] or LIP, was obtained from the relationship [CA–Fe]=ΔF*[CA]t.

RNA extraction: Cells were drained of media and the adherent cells were resuspended in ice-cold 4M Guanidium iso-thiocyanate (GTC) lysis solution. Total RNA was extracted as described by Chomczynski and Sacchi [31], analysed on a 1, 5% denaturing agarose gel for absence of degradation and quantified by UV spectroscopy at 260/280 nm. The RNA, obtained in six different experiments, was used to perform quantitative real time RT-PCR.

cDNA Reverse Transcription (RT) and quantitative real time PCR: One microgram of total RNA was reverse-transcribed using random hexamers and SuperScript III Reverse Transcriptase (Invitrogen, Paisley, UK) according to the manufacturer's instruction. Quantification of PCR products was performed with ABI PRISM 7500 FAST (Thermo Fisher Scientific, USA). The Real Master SYBR Green (Thermo Fisher Scientific, USA) was used to produce fluorescent-labeled PCR products and we monitored increasing fluorescence during repeat cycling of the amplification reaction. Primer sets for all amplicons were designed using the Primer-BLAST software (https://www.ncbi.nlm.nih.gov/ tools/primer-blast). For all primers, the following temperature cycling profile was used: 2 min at 50˚C and 2 min at 95˚C followed by 1 min and 30 s at primer-specific annealing Temperature (for all the primer pairs, the Annealing T was chosen to be around 60˚C, ± 3˚C) for 40 cycles. L34 was used as an internal control because it was shown to be stable with different inductions. The relative level for each gene was calculated using the 2-ΔΔCt method, as depicted in the experimental graphic scheme above (see panel c) (Livak & Schmittgen, 2001).

RNA extraction, cDNA synthesis for q-rt RT-PCR Innate Immune Response MacroArrays: Total RNA was extracted from macrophages by the RNeasy Mini RNA Isolation Kit (Qiagen GmbH, D) 1μg of RNA was reverse transcribed to cDNA by the RT² First Strand Kit (Qiagen Sciences, Maryland, USA). Quantitative RT-PCR was carried out using the ABI7500 Real-Time PCR System and the RT² Profiler™ PCR Array Human Innate and Adaptive Immune Response PCR Array (PAHS-052A, Qiagen). The assay was performed following the producer instructions. Briefly, 25 μl of RT² SYBRGreen/ROX qPCR MasterMix, cDNA (1ml) and RNase-free water were added to each well of the plate, which already contained the forward and reverse primers for the genes of interest: HPRT1, RPL13A, GAPDH and ACTB were used as housekeeping genes. Two replicates of each sample were used and RT-PCR was performed under the following conditions: 95˚C for 10', followed by 40 cycles of 15'' at 95˚C and 1' at 60˚C. For the dissociation curve the profile was 95˚C for 1', 55˚C for 30'' and 95˚C for 30''.

The relative gene expression data was analysed by RT² Profiler PCR Array data analysis v4.0 (Qiagen Superarrays) following the indicated criteria for data validation:

Fold-Regulation represents fold-change results in a biologically meaningful way. Fold-change values greater than one indicates a positive- or an up-regulation, and the fold-regulation is equal to the fold-change;

A: This gene's average threshold cycle is relatively high (> 30) in both the control and the test sample, and is reasonably low in the other sample (< 30). This data means that the gene's expression is relatively low in one sample and reasonably detected in the other sample suggesting that the actual fold-change value is at least as large as the calculated and reported fold-change result. We considered for analysis only genes whose pattern of expression was annotated as A.

B: This gene's average threshold cycle is relatively high (> 30), meaning that its relative expression level is low, in both control and test samples, and the p-value for the fold-change is either unavailable or relatively high ($p > 0.05$).

This fold-change result may also have greater variations; therefore, it is important to have a sufficient number of biological replicates to validate the result for this gene.

C: This gene's average threshold cycle is either not determined or greater than the defined cut-off (default 35), in both samples meaning that its expression was

undetected, making this fold-change result erroneous and un-interpretable.

B. and **C.** RT² Profiler PCR Array data analysis v4.0 scored samples were excluded.

p-values: The p values are calculated based on a Student's t-test of the replicate 2^(- Delta Ct) values for each gene in the control group and treatment groups, and p values less than 0.05 are indicated in red.

Human cytokines protein profiler array: The culture media were collected after 24 hours of infection, upon CpG ODNs treatment. All protein array analyses were performed according to the manufacturer's instructions. Briefly, we blocked membranes with Array Buffer 4 for 1 hour; in the meantime, we prepared samples by adding up to 1 ml of each sample to 0.5 ml of Array Buffer 4, adjusting to a final volume of 1.5 ml with Array Buffer 5. Then we added 15 µl of Cytokines Detection Antibody (which ultimately turns out to be a 1:100 dilution factor) and incubated for 1 hour at room temperature. After that we incubated samples on membranes overnight at 4°C and the day after they were washed with distilled water. We then diluted Streptavidin-HRP in Array Buffer 5 and it was dripped on membranes incubated for 30 minutes at room temperature. After washing each membrane was incubated with chemiluminescent detection reagent.

The culture media were each measured using the Human Cytokine Array Panel A (Proteome Profiler TM) (R&D Systems, Minneapolis, MN, USA). Streptavidin-HPR was used to detect protein expression and the data were captured by exposure to Kodak BioMax Light film by chemiluminescent ECL (Amersham Biosciences, GE Healthcare, UK). The arrays were scanned into a computer and optical density measurements were obtained with Array Vision 7.0 software (Imaging Research Inc., Canada). Positive controls were located in the upper left-hand corner (two spots), lower left-hand corner (two spots) and lower right-hand corner (two spots) of each array kit.

Statistical analyses

Graph Pad Prism 4 (Graph Pad software, San Diego, CA) was used for graphical and statistical analysis. Statistical significance was assessed by analysis of the variance (One Way ANOVA), followed by Bonferroni's post test; the Pearson correlation test was used to find any significant association between the series of values; differences were considered significant at $p < 0.05$.

Results

CpG ODN-treated MDM and *M.tuberculosis* infection

In order to investigate the effect of the new four CpG ODN pre-treatment on the antimicrobial immune response against pathogenic intracellular bacteria, we used an *in vitro* infection model of human monocyte-derived-macrophages (MDMs) infected with H37Rv *Mycobacterium tuberculosis* (MTB) at an Multiplicity of Infection (MOI) of 10.

We treated the cells with each single new CpG for 1 hour, and then we infected with MTB H37Rv. Both MTB infected and untreated cells and GpC treated macrophages were used as negative control. The results of the experiment are summarised in **figure 1A:** the cells pre-treated with CpG3 ODN showed a significantly increased intracellular MTB growth (1,6 fold increase, $p = 0.0003$) while CpG2 ODN treatment reduced the MTB growth (almost 1 LOG, 9.8 fold reduction, $p<0.0001$), as compared to control cells. In respect with the other two new CpG, CpG-1-ODN did not significantly affect MTB growth ($p > 0.05$) while CpG4 induced a less pronounced growth reduction, although statistically significant (5.5 fold reduction, $p = 0.0081$).

To investigate whether flanking sequences missing the immune stimulant TCG 5' and the CTC 3' flanking the CpG motif could influence the biological effects of CpG motif, in particular their anti-mycobacterial activity, we also tested the reverse complement of the four CpG ODNs, having the same hexamer sequence inserted in the reverse complement of previous flanking sequences (referred to as CpG-rev, see supplementary material figure S1). Accordingly, we had CpG1-rev, CpG2-rev, CpG3-rev and CpG4-rev (see table 1 in Math and Meth). The pair CpG3 ODN/CpG3-rev is the only one in which we observed a statistically significant difference in CFU number in that CpG3-rev did not augment the MTB intracellular growth to the same extent as CpG3 ODN. The pair CpG1-ODN/CpG1-rev was not affected by the flanking sequences, indeed also CpG1-ODN did not show a substantial mycobactericidal effect. Data for the pairs CpG2 ODN/CpG2-rev and CpG4-ODN/CpG4-rev were not statistically significant when analyzed with One Way ANOVA, comparing all the data sets together. Nevertheless, when we analyzed the data for each CpG ODN sense *vs.* rev couple, with Mann-Whitney t test, also the differences observed in CpG2- and CpG4-treated cells resulted to be positive (Supplementary figure 1).

CpG ODN-treated MDM and *S.aureus* infection

In order to investigate whether the effect of the new CpG, as well as DNA flanking sequences, was pathogen-dependent we used a second, independent *in vitro* infection model of *S.aureus*, that, compared to MTB, is characterized by a faster replication cycle (roughly 20 minutes *vs* 16 hours) and even if is a class II pathogen represent a bacteria of great interest for nosocomial infection. Interestingly (Figures 1B and 1C) we confirmed, also in *S.aureus* infection model, that the cells pre-treated with CpG3 ODN significantly increased the intracellular bacteria growth, as showed by the rate of increase corresponding to 14,4 fold (1,2 LOG, $p < 0.001$) while CpG2 ODN reduced the growth 19 fold (1.27 LOG, $p < 0.0001$) as compared to control cells.

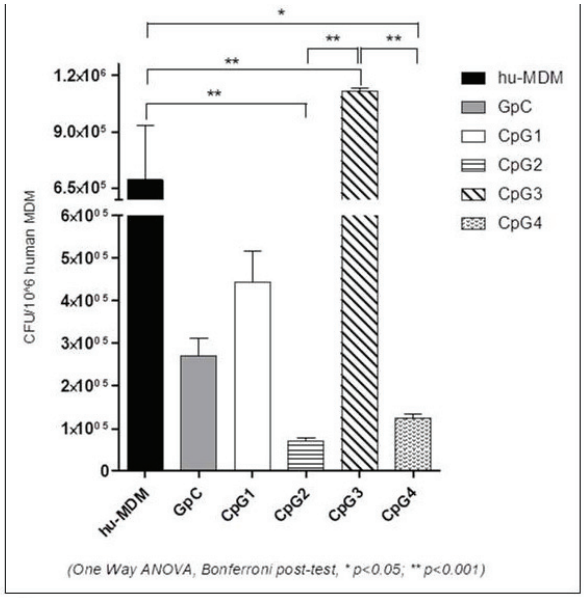

A

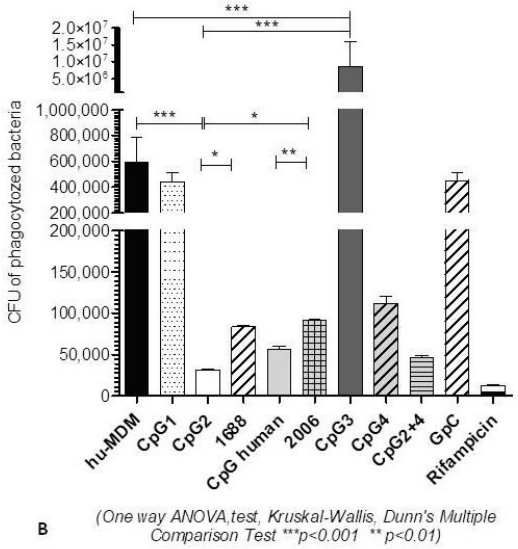

B

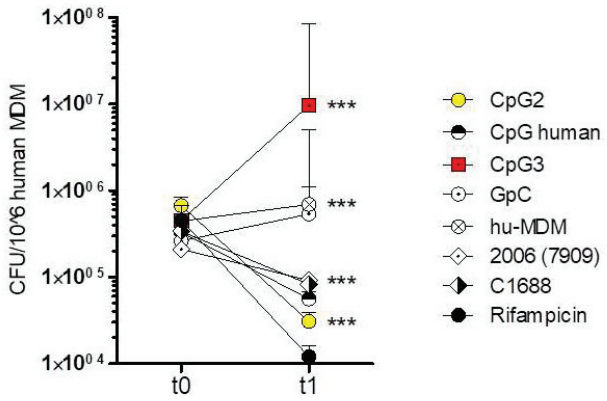

C (One Way ANOVA,Kruskall-Wallis test, *** p<0.001)

	hu-MDM	GpC	CpG2	CpG3	CpG hu	2006	1688	Rifampicin
t1 *vs* t0	2,098	2,028	0,046	30,723	0,174	0,437	0,247	0,027

Figure 1 **A:** MTB CFU in human CpG ODNs pre-treated MDM (1x10^6 cells/well) after 24 hours of infection.
B: *S.aureus* CFU in human CpG ODN pre-treated-MDM after 24 hours of infection.
C: *S.aureus* phagocytosis after 1 hour of MDM CpG ODN treatment and corresponding CFU after 24 hours of infection. The data represent the mean ± sd of the results obtained from experiments performed on ten different donors.

Again, the other two CpG ODN resulted either non-affecting intracellular *S.aureus* growth (as CpG1, $p > 0.05$) or slightly reducing the intracellular bacterial load (as CpG4, 5.2 fold reduction, 0.7 LOG), although statistically significant ($p = 0.018$). Considering the importance of phagocytosis as the first defence response of macrophages, we wondered if the CpG stimulation effect on final replication could depend on the influence of CpG in the initial bacterial entry step. As shown in figure 1C the phagocytosis rate (between 10 to 20% of the initial bacteria administered) did not result significantly influenced by the different CpG, suggesting that the effect identified is due to the subsequent interplay between bacteria and the macrophage response. Indeed, after 24h, CpG 2 ODN is the most stable in reducing CFU, surpassed only by Rifampicin. Comparing the effects between CpG2 and 1688 and CpG human and 2006, we can assume that the hexamer efficiency is also influenced by the flanking sequences.

ipH in hu-MDM plus CpG ODN

It has been demonstrated that the acidification, both endosomal than intracellular, is required for the CpG DNA-mediated leukocyte activation and is coupled to the rapid generation of ROS, which leads to NF-kB activation and subsequent proto-oncogene and cytokine expression [9].

We therefore determined the capacity of the four new CpG ODNs to decrease the MDM intracellular pH (ipH). As shown in figure 2 CpG2 ODN and CpG3 ODN induced a significant decrease of ipH, corresponding to the reduced values of normalized AFU, as compared with the other CpG. CpG1 ODN also induced a ipH decrease, but it was almost overlapping the effect induced by its reverse complement sequence (data not shown) and anyhow not associated to an intracellular bacterial growth decrease.

The decrease of the normalized AFU (Arbitrary Fluorescence Unit) values indicates the lowering of ipH values.

ROS production in MDM treated with CpG ODNs

Following CpG ODNs internalisation the macrophage triggers an orchestrated response, which involves ROS production [9]. We therefore investigated the ROS generation in CpG ODN-treated MDM. As shown in figure 3A, CpG1-ODN and CpG3 ODN treatment significantly increased the ROS generation as compared with control MDM ($p < 0.001$). In MDM treated with CpG4-ODN still a significant increase of ROS was detected *vs*. controls ($p < 0.05$) even if less than CpG1-ODN and CpG3 ODN. Interestingly CpG2 ODN treatment was the only one in which the slightly higher ROS generation, compared to the control, did not result statistically significant.

In view of the opposing immunomodulatory characteristics observed in stimulating the containment of MTB by human MDM, we focused all the subsequent detailed analysis on CpG2 and CpG3 ODNs.

ROS generation in cells involves the catalytic subunit NADPH Oxidase 2 (NOX2), which is encoded by the CYBB (gp91phox) gene, and is the main source of ROS in mononuclear phagocytes and in Polymorphonuclear Leukocytes (PMNs) [32,33]. To ascertain the role of ROS in MTB containment, the CYBB inhibitor DiphenylIodonium (DPI) was added to MDM cultures treated with CpG2 ODN or CpG3 ODN and CFU were counted after 24 hours. As shown in figure 3B, we observed that MTB intracellular growth was reduced in CpG3-treated cells plus DPI, as compared with CpG3 only, while it was ultimately increased in CpG2-treated-MDM plus DPI, even if not statistically significant, as compared with CpG2 only. This finding might suggest that a moderate production of ROS, following MTB infection, is not detrimental *per se*, but that it has to be accurately fine-tuned by the activated MDM, both in timing and amount. Moreover, this data might suggest that CYBB-induced ROS is a necessary factor to contain MTB, but it is not sufficient to regulate the whole process.

Labile Iron Pool (LIP) measurement after CpG2 and CpG3 ODN MDM treatment

The amount of Ferrous or calcein-chelatable, or Labile

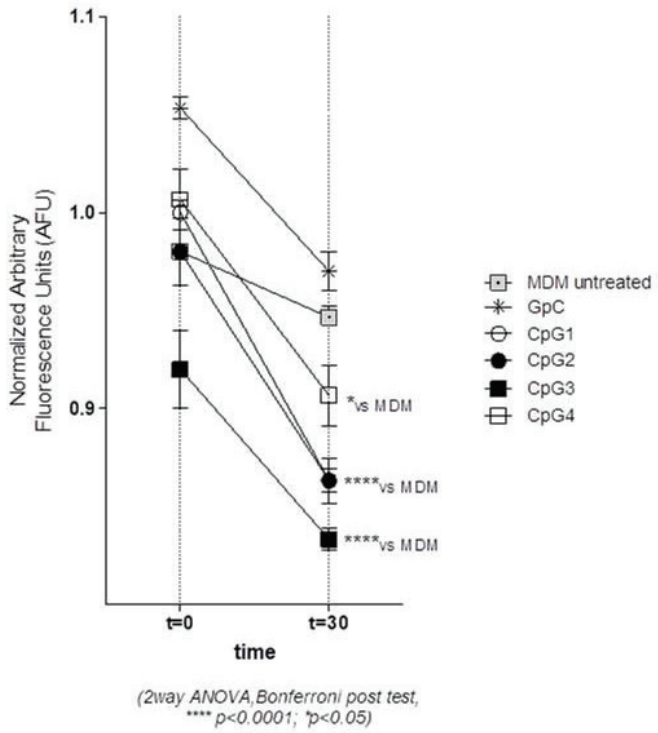

Figure 2 ipH changes in human MDM (1x10^6 cells/well) after CpG ODNs stimulation in a 30 minute time course. The data represent the mean ± sd of the results obtained from experiments performed on five different donors. The decrease of the normalized AFU (Arbitrary Fluorescence Unit) values indicates the lowering of ipH values.

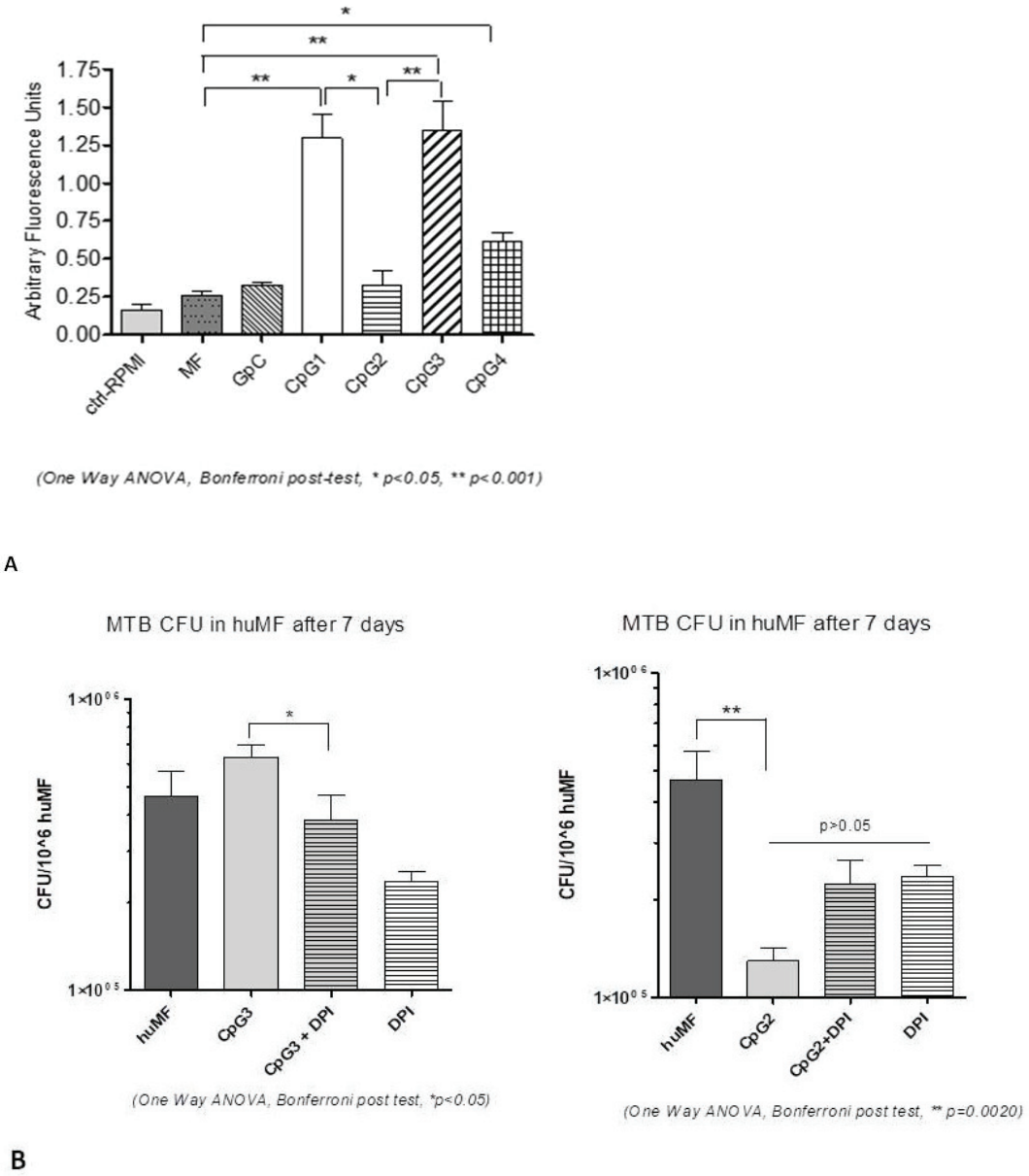

Figure 3 ROS production in human MDM (1x10⁶ cells/well) plus different four CpG ODNs.
A: ROS production in human MDM plus CpG2 and CpG3 ODNs.
B: MTB CFU determination after CpG2 and CpG3 ODNs pre-treatments, with or without CYBB (or gp91 phox) inhibitor DPI co-administration. The data represent the mean ± sd of the results obtained from experiments performed on ten different donors.

Iron (LIP), inside the human MDM it is associated with both ROS production and intracellular mycobacterial growth [20,34].

We measured the amount of LIP in MDM, one hour after CpG2 ODN or CpG3 ODN treatment, to characterise the intracellular environment in which MTB started its replication. In figure 4 we show that only CpG3 ODN increased the amount of Calcein-chelatable LIP, while CpG2 ODN did not affect it. Such an increase might contribute to boost ferrous iron availability to intracellular MTB and, consequently, to enhance the pathogen replication and the ROS pool inside the cells. CA is Calcein, Fe is Iron, [CA-Fe] is the concentration of the Iron-bound CA, [CA] t is the total concentration of intracellular CA, ΔF is the increase in the fluorescence produced by the addition of the chelator Deferiprone. The concentration of iron-bound CA, [CA-Fe] or LIP, was obtained from the relationship [CA–Fe] = ΔF*[CA]t .

Iron homeostasis gene regulation in MDM before and after MTB infection

Considering the role of iron in bacterial replication, we analysed, by q-rt RT-PCR, the relative expression levels

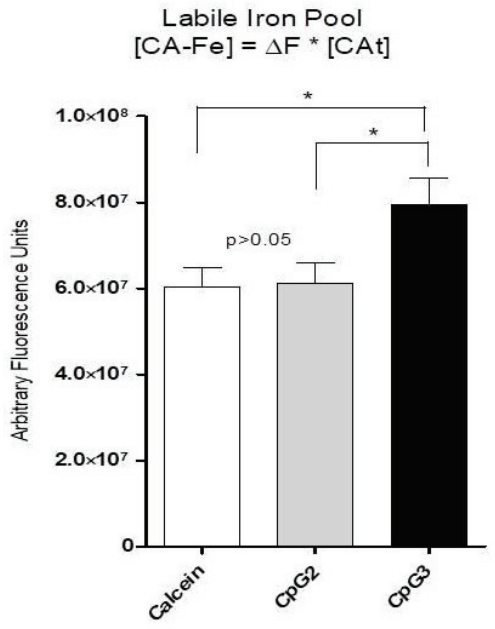

Figure 4 LIP in human MDM plus CpG2 and CpG3 ODNs. Calcein-chelatable Labile Iron Pool (LIP) in human MDM treated with CpG2- and CpG3 ODNs. Fluorescence increases induced by iron chelator were normalised on protein content, assessed by the BCA assay, and considered as LIP values, calculated by the formula: *[CA-Fe]= ΔF * [CAt].* CA is Calcein, Fe is Iron, [CA-Fe] is the concentration of the Iron-bound CA, [CA] t is the total concentration of intracellular CA, and DF is the increase in the fluorescence produced by the addition of the chelator Deferiprone. The concentration of iron-bound CA,[CA-Fe] or LIP, was obtained from the relationship [CA−Fe]=ΔF*[CA]t
The data represent the mean ± sd of the results obtained from experiments performed on ten different donors.

of a group of iron regulating genes, mainly involved in the macrophage response to infection, such as Transferrin receptor 1 (TfR1), Ferritin Heavy chain (Ferr H), Heme Oxygenase 1 (HOX1), Ferroportin (Fp) and Nramp1. The main function of these genes is depicted in the graphical cartoon in figure 5. Briefly, TfR1 mediates Transferrin (Tf) bound Iron in the cells, FerrH stores ferric iron in the lysosome, Ferroportin export iron outside the cells, while Nramp1 antiport mediates iron entry in the phagolysosome and H+ exit (and viceversa). HOX1 degrades free Heme and produces iron, biliverdin and Carbon Monoxide (CO).

The relative gene expression of CpG ODN-treated MDM was analysed before and after 24 hours of MTB infection.

Before MTB infection (Figure 5 top panel), the treatment with CpG2 ODN induced statistically significant differences for Nramp1 and TfR1 genes expression, both of them being induced (fold-induction >1.9), as compared with nearly unchanged expression in CpG3-MDMs. Fp and HOX1 were similarly induced by the two CpG ODN treatments, while Ferr H showed a tendency to be repressed by CpG2 ODN (fold-induction <0.5).

After MTB infection (Figure 5 central panel) the expression levels of Nramp1 and HOX1 were further enhanced in CpG2 ODN-MDM, while they became no longer detectable in CpG3 ODN-MDM, together with Ferr H, being it now induced by CpG2 ODN. Interestingly, MTB-infected MDMs showed TfR1 repressed by CpG2- and induced by CpG3 ODN, while Fp no longer showed differences *vs.* control cells in both the treatments.

Overall CpG2 treatment induced in MTB-infected MDM an Iron retention or "compartmentalisation" phenotype while CpG3 ODN MDM showed an iron release phenotype.

By strictly regulating the localisation and protein binding of Labile Iron, CpG2 might help the MDM to deprive the intracellular pathogen of this precious mineral.

Innate immune response gene array: To further characterize the MDM intracellular milieu encountered by MTB in the initial phase of infection, i.e. after 1 hour of CpG ODN treatment, we broadened the analysis of CpG ODN effects to a larger group of genes orchestrating the Innate Immune response, by means of RT-macroarrays with 84 genes belonging to this pathway. A group of nine genes was induced by both the CpG ODNs (not shown), namely: TGF-β, FNγR2, β2 Microglobulin, CD55, IL1RAP, IL-10, CYBB, IκBκB and IL-36B.

Remarkably (Figure 6), two genes, PPBP and IL-36RN, were induced only by CpG3 ODN (in CpG2-MDM the first being unchanged and the second not even detectable). The genes: IL-1B, IL-1R2, CCR3, CD14 and NF-κB2 resulted repressed only by CpG3 ODN, while they stayed unchanged in CpG2-MDM. In contrast, TRAF6 and NLRC4 were induced only by CpG2 ODN, and were, respectively, unchanged and repressed in CpG3-MDM. Finally, two relevant genes for innate immune response, TREM1 and CHUK, were repressed solely by CpG2 ODN.

Protein released in MDM supernatants: We finally examined the effects of CpG ODN-treatment on MDM response to MTB infection in terms of protein release in cell Supernatants (SNs). A group of four proteins was released by infected MDM treated with either of the two CpG ODNs: TNF-alpha, IL-8, IL-6 and IL-1RN (Figure 7). Interestingly, and somehow unexpectedly, we found that only in the SNs of CpG2 ODN-treated MDMs another group of proteins was released, most of them being chemokines clustered on 4q and 17q arms of their respective chromosomes, many of which are IL-1B-regulated: CCL1, CCL2, CCL3, CCL4, CCL5, CXCL1, CXCL10, CXCL11. CpG2-MDM SN contained also CXCL12, G-CSF, GM-CSF, IL-27, PAI1, and, importantly, soluble TREM1 (sTREM1), the soluble isoform of the Triggering Receptor Expressed on Myeloid cells 1, a potential regulator of myeloid activation [35].

Discussion

Our study focused on MTB infection of human MDMs to verify whether the treatment with CpG ODN might improve

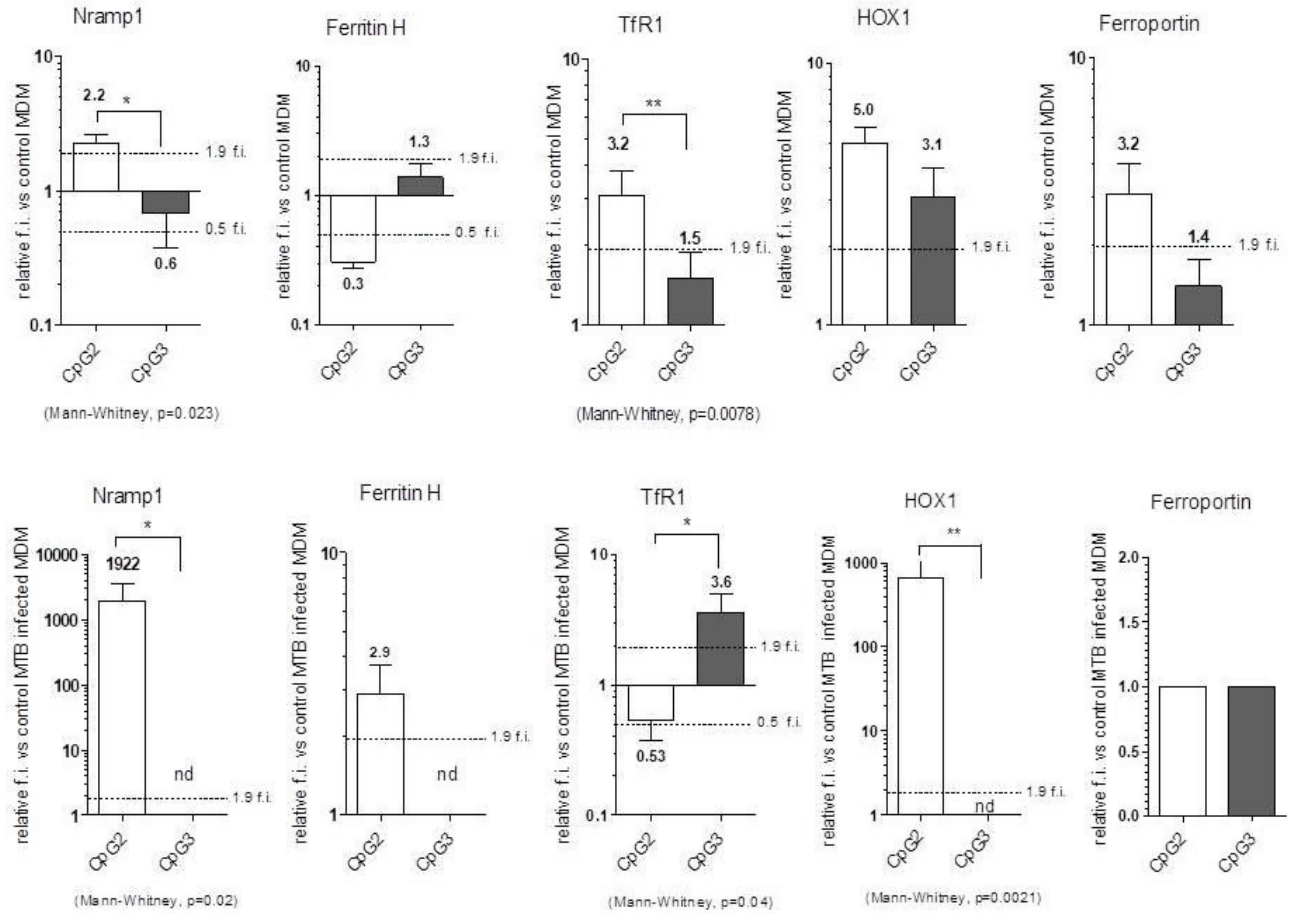

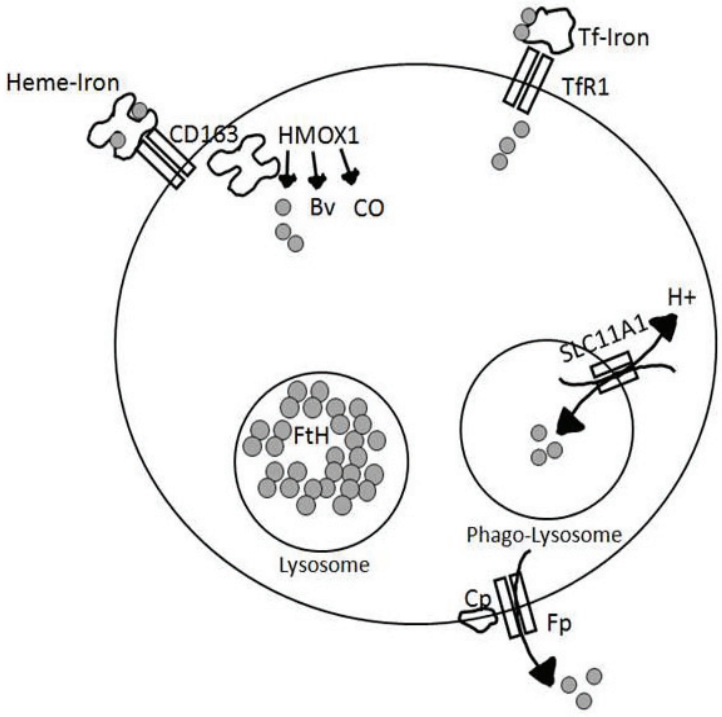

Figure 5 Iron homeostasis gene regulation in human MDM before (upper panel) and after MTB infection (bottom panel), by specific primers q-rt RT-PCR. Pre-treated CpG ODN MDMs are compared to untreated MDM of the very same donor, while pre-treated and MTB infected MDMs are compared to untreated MTB infected MDM of the very same donor. The data represent the mean ± sd of the results obtained from experiments performed on ten different donors, normalized on L34 gene expression.

Gene	CpG2	CpG3	Gene function
PPBP	-1	2,2	Chemoattractant and activator of neutrophils, formation and secretion of plasminogen activator
IL-36RN	nd	2,9	Interleukin-1 receptor antagonist,
NLRC4	1,9	1,5	NLR family, CARD domain containing 4; plays a role in the promotion of apoptosis
TRAF6	1,9	-2,7	Member of the TNF receptor associated factor (TRAF) protein family.
IL1B	-1,6	-2	Important mediator of the inflammatory response, is involved in a variety of cellular activities, including cell proliferation, differentiation, and apoptosis.
IL1R2	-1,3	-2,2	Non-signaling receptor for IL1A, IL1B and IL1RN.
CCR3	-1,6	-2,1	Binds to RANTES, and subsequently transduces a signal by increasing the intracellular calcium ions level
CD14	1,6	-1,9	In concert with LBP, binds to monomeric LPS and delivers it to the MD-2/TLR4 complex, thereby mediating the innate immune response to bacterial LPS.
NFkB2	-1,2	-2,9	NFKB2 appears to have dual functions such as cytoplasmic retention of attached NF-kappa-B proteins by p100 and generation of p52 by a cotranslational processing.
CHUK	-3,6	-1,3	IKKalpha
TREM1	-3,4	-1,3	This protein amplifies neutrophil and monocyte-mediated inflammatory responses triggered by bacterial and fungal infections by stimulating release of pro-inflammatory chemokines and cytokines, as well as increased surface expression of cell activation markers.

>1,9	HK	<-1,9

Figure 6 RT2 profiler Macroarrays for Innate Immune Response. Total CpG-ODN-treated MDM RNA, from 3 different donors, was reverse-transcribed to cDNA and subjected to q-rt RT-PCR specific for 83 genes involved in innate response. Genes with fold-regulation higher than 1.9 were considered induced (red), those with fold-regulation lower than -1.9 were considered repressed (green), and those comprised between 1.9 and -1.9 were considered unchanged vs. untreated MDMs. In the analysis we chose to include only the genes classified as "A" by the software analysis file, i.e.: this gene's average threshold cycle is relatively high (> 30) in either the control or the test sample, and is reasonably low in the other sample (< 30).
HK stays for Housekeeping, i.e. non changing above or below the indicated range of fold-induction.

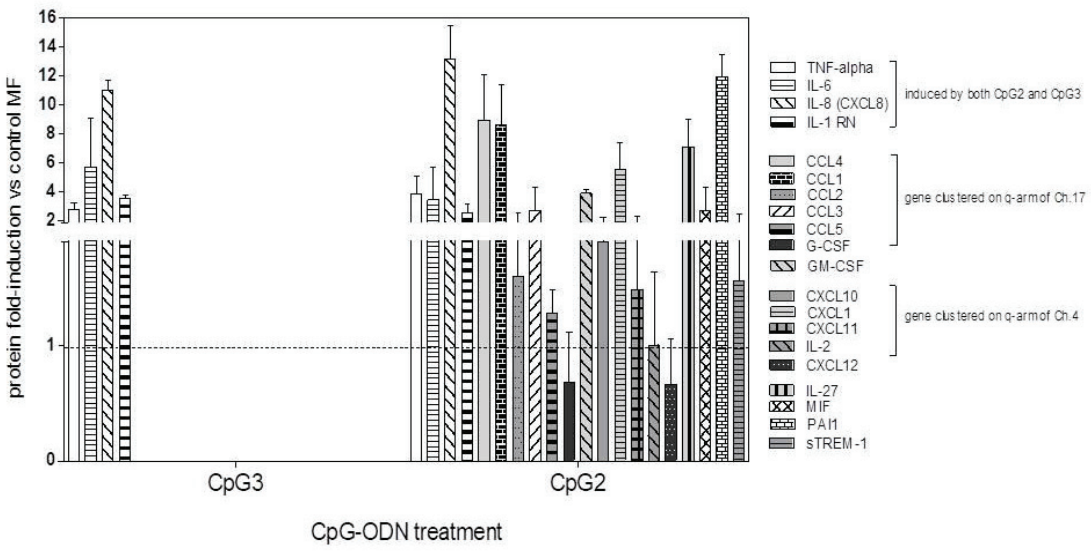

Figure 7 Protein profiler array analysis of proteins released in cells SNs by CpG ODN-treated human MDM infected (1x10^6 cells/treatment) with *M. tuberculosis* after 24 hours of infection. The protein array has been performed on 3 different donors and each protein has been detected in duplicate.

their ability to contain MTB. We tested four newly designed CpG ODN (Table 1A) and lastly chose CpG2 and CpG3, which gave opposite results in MTB infection containment, in order to highlight their different effects on intracellular settings of cells infected after CpG ODN treatment.

We also confirmed the same effect in a second, independent and separate model of bacterial infection using *S.aureus*. CpG2 ODN-treatment of MDMs induced an increased containment of both MTB and *S.aureus* intracellular growth, while CpG3 one resulted in increased intracellular

CFU of both the pathogens, suggesting that the CpG effect is independent from the growth rate of the bacteria.

CpG2 motif has already been used in other studies, though with different sequence scaffolds, and it has been shown to induce ROS production in murine macrophage-like cell line RAW264.7 [36]. In our study, we inserted the CpG2 motif in different flanking region and phosphodiester backbone. Differently, as far as we know, the CpG3 motif was never employed to stimulate human MDM.

Of note, CpG3 motif, when inserted in the "wrong" flanking sequence, i.e. the reverse complement of the initial one, loses almost completely its potent pro-inflammatory effect, while this is not true for all the other three CpG ODNs. As previously demonstrated, the acidification, both endosomal and intracellular, is required for the CpG DNA-mediated leukocyte activation and is coupled to the rapid generation of ROS [9].

In agreement with these finding, we were able to demonstrate that both CpG2-ODN and CpG3-ODN induced a significant decrease of ipH in human MDMs while the increase of ROS production are induced only by CpG3 ODN treatment.

CpG2 ODN induced only a slight increase of ROS production in human MDMs. Conversely, we observed a five-fold higher ROS production induced by CpG3 ODN, associated with an increased MTB intracellular growth. This is in agreement with the previous demonstration that an uncontrolled oxidative burst following infection is detrimental for human phagocytes [37] and might produce favourable results for intracellular pathogens. The production of ROS following MTB infection, not damaging *per se*, has to be accurately kept under control by the activated MDM. As a matter of fact, when we treated MDM with CpG2-ODN and then inhibited ROS production with DPI (the inhibitor of gp91phox), we got a higher MTB growth. On the other hand, when we did the same in CpG3 ODN-MDM, we got a significant MTB growth reduction.

We could then draw the conclusion that the slight ROS increase induced by CpG2 ODN is necessary and possibly, in the correct intracellular milieu, sufficient to affect MTB intracellular growth, while the abundant ROS production induced by CpG3 ODN might eventually trigger an uncontrolled oxidative burst in infected MDMs damaging the cells and possibly favouring MTB intracellular growth. It is well established that the growth and pathogenicity of MTB is strong linked on a sufficient supply of iron [38]. Mycobacteria are able to acquire iron through multiple avenues including: the acquisition of the metal from transferrin, by directly binding iron-loaded transferrin via specific receptors, by uptake of cytoplasmic iron or heme iron, by the production of siderophores.

In this respect, we found that treatment with CpG3-ODN increased the amount of labile, or ferrous iron in MDM, while CpG2 ODN-MDM did not differ from controls. Iron is an essential component in cellular metabolism of both eukaryotic and prokaryotic cells. During the course of infection host cells and intracellular pathogens compete for its availability, which may determine the outcome of macrophages infection by pathogens like MTB.

The iron homeostasis is tightly controlled by a number of genes, and there is now a reasonable agreement on the fact that iron trafficking and metabolism contribute to macrophages polarised phenotype. It is also well documented that, in presence of ROS, ferrous Iron contributes to increase the oxidative burst of the cells by the Fenton's reaction [39].

We therefore evaluated the expression of genes involved in iron metabolism to highlight the existence of possibly induced iron retention/release phenotypes. Firstly, we estimated the expression level of the genes TfR1, Nramp1, HMOX1, FerrH and Fp one hour after CpG ODN treatment, in order to probe the intracellular milieu found by the pathogen upon entry in MDM. We then repeated the measurement 24 hours after MTB infection, to describe the complex interplay between MDM and intracellular MTB during the infection. Our results showed that CpG2-ODN pre-treatment induced an Iron retention phenotype, while CpG3 ODN triggered an Iron release one [39]. In particular two genes, namely HOX1 and Nramp1, appeared to be tightly regulated by CpG2 ODN in MTB infection. Nramp1, a divalent cation/H+ antiport membrane protein, might had either deprived the intra-phagosomal MTB of iron, or removed the free Iron from cytosol and transported it in the phagolysosome to kill MTB with the Fenton's reaction products (as it could be suggested by the steady state LIP in CpG2-MDM), in both cases helping the mycobactericidal activity of MDMs.

HMOX-1 is an inducible immunomodulatory [40] and cytoprotective enzyme [41] whose fundamental purpose is the degradation of Heme to biliverdin, Carbon Monoxide (CO), both of them anti-oxidants, and free iron [42]. Wegiel recently proposed that when CO is endogenously produced by HMOX-1, it acts as a key mediator of host defence used by the macrophages [43]. The strong induction of HMOX-1 following MTB infection of MDM was observed exclusively after CpG2 ODN treatment and we suppose that it could have enhanced the cells capacity to kill MTB. In this respect, HMOX-1 expression in MTB-infected macrophages has been already shown in mice [44] and an important role for HMOX-1 in controlling MTB in human macrophages has been recently proposed [45]. At the same time, HMOX-1 expression in MTB-infected CpG2-pre-treated MDM might also have contributed to "dampen" innate response, thus exerting its proposed cytoprotective and anti-inflammatory action [46].

Further investigations on Nramp1 and HOX-1 modulation of iron metabolism role in innate MDM response vs. MTB

infection might provide useful information to possibly exploit the so called "nutritional immunity" of the host in the battle for iron with intracellular pathogens.

In innate immunity, while it is clearly established that CpG motifs play a PAMP role, we wondered whether they might also play a DAMP signal, being hypothetically present in mitochondrial DNA. It was hypothesized that mitochondria probably evolved from a bacterial ancestor establishing a symbiotic relationship with its host cell and, in this regard, mitochondrial DAMPs (or mDAMPs) can be viewed as intermediate entities between DAMPs and PAMPs [47]. Evidence is accumulating that TLR9 not only recognizes CpG motifs in bacterial DNA but also similar motifs in vertebrate DNA. In this respect, the same receptor recognizes PAMP and DAMP, which follows the concept that the immune system is more concerned with entities that do damage than those that are foreign [48].

Since CpG2 sequence is found both in MTB and human mitochondrial DNA (not shown), it could hypothetically work, at the same time, as a PAMP and a DAMP signal for human MDM, therefore constituting a double signal of activation. On the contrary, CpG3 motif, mostly absent in human mitochondrial DNA, but well represented in MTB genome, stimulates human MDM as a classical PAMP, inducing ROS production and iron release, possibly due to the oxidative burst damage of Ferritin-stored Iron.

A very important issue regarding human innate immunity is how to obtain the best response from the host's cells, in terms of accurate phasing and timing of responses to DAMPs or PAMPs, in order to avoid the detrimental burden of inflammation while, instead, being able to contain either tissue damage or bacterial infection [49]. Therefore, it is tempting to speculate that CpG2-ODN would prompt MDM to react more appropriately to two signals: it is necessary to face an intracellular infection (PAMP) and a tissue damage (DAMP). In this way the treated cells would be equipped with a rapid and intense response to MTB entry (as provided by NCLC4 inflammasome activation and TRAF6 signalling induction before MTB entry, and, afterwards, by an orchestrated array of cytokines and chemokines), but always keeping under control oxidative burst and inflammatory response intensity.

In this scenario the CpG2-mediated down-regulation of TREM1, and the subsequent release of soluble TREM1 (sTREM1), after MTB infection, could have played a regulatory role, together with PAI1 release, and restored homeostasis in cells, as described by a comprehensive insight review on the several control points in inflammation [49].

TREM1 is a DAP12 associated receptor, which is up-regulated in response to LPS-mediated TLR4 activation, and plays an essential role in innate immune response by augmenting the production of pro-inflammatory chemokines and cytokines, while its soluble form (sTREM-1) exerts anti-inflammatory effects [50].

PAI1 is the plasminogen activator inhibitor 1 and hence is an inhibitor of fibrinolysis and ECM degradation in the MDM surroundings. Of note, it has been recently reported that molecules of the fibrinolytic system are up-regulated in the chronic phase of experimental tuberculosis and it was suggested that the mycobacterium itself could play an important role in the over expression of molecules of the fibrinolytic system, contributing to chronic inflammation in tuberculosis [51]. Moreover, PAI1 has been also described to be an iron-responsive protein, in a study in which the authors evidenced a dose-dependent increase in PAI-1 antigen levels expressed in cells treated with deferoxamine, an iron chelator.

At MTB entry in CpG3 ODN-MDM, the pathogen finds an intracellular milieu rich of the metabolically active Ferrous Iron, further increased by the Fenton's reaction triggered by ROS production, which facilitates its intracellular growth. In such a scenario, the induction of PPBP, generating inflammation (glycolysis, intracellular cAMP accumulation, prostaglandin E2 secretion, and synthesis of hyaluronic acid http://www.genecards.org), does not help the MDM to kill intracellular MTB. The other gene induced by CpG3 ODN, IL36RN, is a highly and specific antagonist of the IL-1 receptor-related protein 2/IL1RL2-mediated response to interleukin IL36G and IL-1B (http://www.genecards.org). IL-1 is not only triggered by infectious danger signals but also by danger signals released from metabolically 'stressed' or even dying cells. CpG3 ODN represses in MDM the IL1-B and IL-1R2 expression and inhibits their signalling by IL36-RN, therefore inhibiting the danger signals to pre-activate the cells. Together with TRAF6 down regulation such a pattern depicts a human MDM phenotype not only characterised by an uncontrolled oxidative burst but also characterised by an incomplete inflammatory response, which is unable to mount a rapid and protective mycobactericidal response.

As opposite, CpG2 ODN immediately triggers a fully activated MDM phenotype, able to keep under strict control ROS, free Iron and ECM degradation, and, perhaps just for this reason, these MDMs end up with well equipped mycobactericidal power.

The possibility to include the new identified phosphodiester CpG ODN in delivery system, overcoming the intracellular degradation, improving the cellular uptake and delivering the CpG to the target tissue, make them an interesting candidate for future clinical application.

Author Contributions

DG, AB, FA, GC and AS, performed the experiments and took part in planning the experiments and analysed the data. VC helped in fund raising and discussed the data, FM

planned the experiments, supervised the work and wrote the paper, with the critical reading of GC and DG.

Acknowledgment

Funding information

This research was funded by National Research Council, Project: Nutrizione, Alimentazione & Invecchiamento Attivo, (NUTR-AGE), Tasks 4.2 and 4.3.

Conflict of interest

The authors declared that there is no conflict of interests regarding the publication of this manuscript.

References

1. Liu J, Wei Y, Lu Y, Li Y, Chen Q, Li Y. The discovery of potent immunostimulatory CpG-ODNs widely distributed in bacterial genomes. J Microbiol. 2020 Feb;58(2):153-162. doi: 10.1007/s12275-020-9289-y. Epub 2019 Dec 23. Erratum in: J Microbiol. 2020 Apr;58(4):340. PMID: 31872374.
2. Krieg AM, Love-Homan L, Yi AK, Harty JT. CpG DNA induces sustained IL-12 expression in vivo and resistance to Listeria monocytogenes challenge. J Immunol. 1998 Sep 1;161(5):2428-34. PMID: 9725240.
3. Ito S, Ishii KJ, Ihata A, Klinman DM. Contribution of nitric oxide to CpG-mediated protection against Listeria monocytogenes. Infect Immun. 2005 Jun;73(6):3803-5. doi: 10.1128/IAI.73.6.3803-3805.2005. PMID: 15908417; PMCID: PMC1111823.
4. Ito S, Ishii KJ, Shirota H, Klinman DM. CpG oligodeoxynucleotides improve the survival of pregnant and fetal mice following Listeria monocytogenes infection. Infect Immun. 2004 Jun;72(6):3543-8. doi: 10.1128/IAI.72.6.3543-3548.2004. PMID: 15155663; PMCID: PMC415688.
5. Zimmermann S, Egeter O, Hausmann S, Lipford GB, Röcken M, Wagner H, Heeg K. CpG oligodeoxynucleotides trigger protective and curative Th1 responses in lethal murine leishmaniasis. J Immunol. 1998 Apr 15;160(8):3627-30. PMID: 9558060.
6. Elkins KL, Rhinehart-Jones TR, Stibitz S, Conover JS, Klinman DM. Bacterial DNA containing CpG motifs stimulates lymphocyte-dependent protection of mice against lethal infection with intracellular bacteria. J Immunol. 1999 Feb 15;162(4):2291-8. PMID: 9973506.
7. Kim TH, Kim D, Gautam A, Lee H, Kwak MH, Park MC, Park S, Wu G, Lee BL, Lee Y, Kwon HJ. CpG-DNA exerts antibacterial effects by protecting immune cells and producing bacteria-reactive antibodies. Sci Rep. 2018 Nov 2;8(1):16236. doi: 10.1038/s41598-018-34722-y. PMID: 30390012; PMCID: PMC6214913.
8. Greco E, Santucci MB, Quintiliani G, Papi M, De Spirito M, Fraziano M. CpG oligodeoxynucleotides promote phospholipase D dependent phagolysosome maturation and intracellular mycobacterial killing in M. tuberculosis infected type II alveolar epithelial cells. Cell Immunol. 2009;259(1):1-4. doi: 10.1016/j.cellimm.2009.06.002. Epub 2009 Jun 6. PMID: 19560127.
9. Yi AK, Tuetken R, Redford T, Waldschmidt M, Kirsch J, Krieg AM. CpG motifs in bacterial DNA activate leukocytes through the pH-dependent generation of reactive oxygen species. J Immunol. 1998 May 15;160(10):4755-61. PMID: 9590221.
10. Hartmann G, Weiner GJ, Krieg AM. CpG DNA: a potent signal for growth, activation, and maturation of human dendritic cells. Proc Natl Acad Sci U S A. 1999 Aug 3;96(16):9305-10. doi: 10.1073/pnas.96.16.9305. PMID: 10430938; PMCID: PMC17777.
11. Hartmann G, Weeratna RD, Ballas ZK, Payette P, Blackwell S, Suparto I, Rasmussen WL, Waldschmidt M, Sajuthi D, Purcell RH, Davis HL, Krieg AM. Delineation of a CpG phosphorothioate oligodeoxynucleotide for activating primate immune responses in vitro and in vivo. J Immunol. 2000 Feb 1;164(3):1617-24. doi: 10.4049/jimmunol.164.3.1617. PMID: 10640783.
12. Freidag BL, Melton GB, Collins F, Klinman DM, Cheever A, Stobie L, Suen W, Seder RA. CpG oligodeoxynucleotides and interleukin-12 improve the efficacy of Mycobacterium bovis BCG vaccination in mice challenged with M. tuberculosis. Infect Immun. 2000 May;68(5):2948-53. doi: 10.1128/IAI.68.5.2948-2953.2000. PMID: 10768993; PMCID: PMC97508.
13. Juffermans NP, Leemans JC, Florquin S, Verbon A, Kolk AH, Speelman P, van Deventer SJ, van der Poll T. CpG oligodeoxynucleotides enhance host defense during murine tuberculosis. Infect Immun. 2002 Jan;70(1):147-52. doi: 10.1128/IAI.70.1.147-152.2002. PMID: 11748176; PMCID: PMC127605.
14. Hanagata N. Structure-dependent immunostimulatory effect of CpG oligodeoxynucleotides and their delivery system. Int J Nanomedicine. 2012;7:2181-95. doi: 10.2147/IJN.S30197. Epub 2012 Apr 27. PMID: 22619554; PMCID: PMC3356174.
15. Pohar J, Lainšček D, Kunšek A, Cajnko MM, Jerala R, Benčina M. Phosphodiester backbone of the CpG motif within immunostimulatory oligodeoxynucleotides augments activation of Toll-like receptor 9. Sci Rep. 2017 Nov 6;7(1):14598. doi: 10.1038/s41598-017-15178-y. Erratum in: Sci Rep. 2018 Jan 5;8(1):355. Erratum in: Sci Rep. 2018 Mar 6;8(1):4269. PMID: 29097808; PMCID: PMC5668283.
16. Zimmermann S, Heeg K, Dalpke A. Immunostimulatory DNA as adjuvant: efficacy of phosphodiester CpG oligonucleotides is enhanced by 3' sequence modifications. Vaccine. 2003 Feb 14;21(9-10):990-5. doi: 10.1016/s0264-410x(02)00550-9. PMID: 12547613.
17. Mellman I, Fuchs R, Helenius A. Acidification of the endocytic and exocytic pathways. Annu Rev Biochem. 1986;55:663-700. doi: 10.1146/annurev.bi.55.070186.003311. PMID: 2874766.
18. Sen CK, Packer L. Antioxidant and redox regulation of gene transcription. FASEB J. 1996 May;10(7):709-20. doi: 10.1096/fasebj.10.7.8635688. PMID: 8635688.
19. Yi AK, Chace JH, Cowdery JS, Krieg AM. IFN-gamma promotes IL-6 and IgM secretion in response to CpG motifs in bacterial DNA and oligodeoxynucleotides. J Immunol. 1996 Jan 15;156(2):558-64. PMID: 8543806.
20. Bresgen N, Eckl PM. Oxidative stress and the homeodynamics of iron metabolism. Biomolecules. 2015 May 11;5(2):808-47. doi: 10.3390/biom5020808. PMID: 25970586; PMCID: PMC4496698.
21. Gackowski D, Kruszewski M, Bartlomiejczyk T, Jawien A, Ciecierski M, Olinski R. The level of 8-oxo-7,8-dihydro-2'-deoxyguanosine is positively correlated with the size of the labile iron pool in human lymphocytes. J Biol Inorg Chem. 2002 Apr;7(4-5):548-50. doi: 10.1007/s00775-001-0335-x. Epub 2002 Jan 30. PMID: 11941513.
22. Corna G, Campana L, Pignatti E, Castiglioni A, Tagliafico E, Bosurgi L, Campanella A, Brunelli S, Manfredi AA, Apostoli P, Silvestri L, Camaschella C, Rovere-Querini P. Polarization dictates iron handling by inflammatory and alternatively activated macrophages. Haematologica. 2010 Nov;95(11):1814-22. doi: 10.3324/haematol.2010.023879. Epub 2010 May 29. PMID: 20511666; PMCID: PMC2966902.
23. Recalcati S, Locati M, Cairo G. Systemic and cellular consequences of macrophage control of iron metabolism. Semin Immunol. 2012 Dec;24(6):393-8. doi: 10.1016/j.smim.2013.01.001. Epub 2013 Jan 30. PMID: 23375134.
24. Molad Y, Pokroy-Shapira E, Carmon V. CpG-oligodeoxynucleotide-induced TLR9 activation regulates macrophage TREM-1 expression and shedding. Innate Immun. 2013 Dec;19(6):623-30. doi: 10.1177/1753425913476970. Epub 2013 Mar 8. PMID: 23475790.
25. Yu D, Kandimalla ER, Zhao Q, Bhagat L, Cong Y, Agrawal S. Requirement of nucleobase proximal to CpG dinucleotide for immunostimulatory activity of synthetic CpG DNA. Bioorg Med Chem. 2003 Feb 6;11(3):459-64. doi: 10.1016/s0968-0896(02)00430-3. PMID: 12517441.
26. Nathan C, Ding A. Nonresolving inflammation. Cell. 2010 Mar 19;140(6):871-82. doi: 10.1016/j.cell.2010.02.029. PMID: 20303877.
27. Krieg AM. CpG motifs in bacterial DNA and their immune effects. Annu Rev Immunol. 2002;20:709-60. doi: 10.1146/annurev.immunol.20.100301.064842. Epub 2001 Oct 4. PMID: 11861616.
28. Grinstein S, Cohen S, Goetz-Smith JD, Dixon SJ. Measurements of cytoplasmic pH and cellular volume for detection of Na+/H+ exchange in lymphocytes. Methods Enzymol. 1989;173:777-90. doi: 10.1016/s0076-6879(89)73050-0. PMID: 2550736.
29. Greco E, Quintiliani G, Santucci MB, Serafino A, Ciccaglione AR, Marcantonio C, Papi M, Maulucci G, Delogu G, Martino A, Goletti D, Sarmati L, Andreoni M, Altieri A, Alma M, Caccamo N, Di Liberto D, De Spirito M, Savage ND, Nisini R, Dieli F, Ottenhoff TH, Fraziano M. Janus-faced liposomes enhance antimicrobial innate immune response in Mycobacterium tuberculosis infection. Proc Natl Acad Sci U S A. 2012 May 22;109(21):E1360-8. doi: 10.1073/pnas.1200484109. Epub 2012 Apr 25. PMID: 22538807; PMCID: PMC3361443.
30. Epsztejn S, Kakhlon O, Glickstein H, Breuer W, Cabantchik I. Fluorescence analysis of the labile iron pool of mammalian cells. Anal Biochem. 1997 May 15;248(1):31-40. doi: 10.1006/abio.1997.2126. PMID: 9177722.
31. Chomczynski P, Sacchi N. Single-step method of RNA isolation by acid guanidinium

thiocyanate-phenol-chloroform extraction. Anal Biochem. 1987 Apr;162(1):156-9. doi: 10.1006/abio.1987.9999. PMID: 2440339.

32. Adachi Y, Kindzelskii AL, Petty AR, Huang JB, Maeda N, Yotsumoto S, Aratani Y, Ohno N, Petty HR. IFN-gamma primes RAW264 macrophages and human monocytes for enhanced oxidant production in response to CpG DNA via metabolic signaling: roles of TLR9 and myeloperoxidase trafficking. J Immunol. 2006 Apr 15;176(8):5033-40. doi: 10.4049/jimmunol.176.8.5033. PMID: 16585600.

33. Nathan C, Cunningham-Bussel A. Beyond oxidative stress: an immunologist's guide to reactive oxygen species. Nat Rev Immunol. 2013 May;13(5):349-61. doi: 10.1038/nri3423. PMID: 23618831; PMCID: PMC4250048.

34. Ratledge C. Iron, mycobacteria and tuberculosis. Tuberculosis (Edinb). 2004;84(1-2):110-30. doi: 10.1016/j.tube.2003.08.012. PMID: 14670352.

35. Gingras MC, Lapillonne H, Margolin JF. TREM-1, MDL-1, and DAP12 expression is associated with a mature stage of myeloid development. Mol Immunol. 2002 Mar;38(11):817-24. doi: 10.1016/s0161-5890(02)00004-4. PMID: 11922939.

36. Kirsch JD, Yi AK, Spitz DR, Krieg AM. Accumulation of glutathione disulfide mediates NF-kappaB activation during immune stimulation with CpG DNA. Antisense Nucleic Acid Drug Dev. 2002 Oct;12(5):327-40. doi: 10.1089/108729002761381302. PMID: 12477282. Nathan C, Shiloh MU. Reactive oxygen and nitrogen intermediates in the relationship between mammalian hosts and microbial pathogens. Proc Natl Acad Sci U S A. 2000 Aug 1;97(16):8841-8. doi: 10.1073/pnas.97.16.8841. PMID: 10922044; PMCID: PMC34021.

37. Olakanmi O, Schlesinger LS, Ahmed A, Britigan BE. Intraphagosomal Mycobacterium tuberculosis acquires iron from both extracellular transferrin and intracellular iron pools. Impact of interferon-gamma and hemochromatosis. J Biol Chem. 2002 Dec 20;277(51):49727-34. doi: 10.1074/jbc.M209768200. Epub 2002 Oct 23. PMID: 12399453.

38. Cairo G, Recalcati S, Mantovani A, Locati M. Iron trafficking and metabolism in macrophages: contribution to the polarized phenotype. Trends Immunol. 2011 Jun;32(6):241-7. doi: 10.1016/j.it.2011.03.007. Epub 2011 Apr 21. PMID: 21514223. Panther E, Dürk T, Ferrari D, Di Virgilio F, Grimm M, Sorichter S, Cicko S, Herouy Y, Norgauer J, Idzko M, Müller T. AMP affects intracellular Ca2+ signaling, migration, cytokine secretion and T cell priming capacity of dendritic cells. PLoS One. 2012;7(5):e37560. doi: 10.1371/journal.pone.0037560. Epub 2012 May 18. PMID: 22624049; PMCID: PMC3356328.

39. Russell DG, Cardona PJ, Kim MJ, Allain S, Altare F. Foamy macrophages and the progression of the human tuberculosis granuloma. Nat Immunol. 2009 Sep;10(9):943-8. doi: 10.1038/ni.1781. Epub 2009 Aug 19. PMID: 19692995; PMCID: PMC2759071. Kaufmann A, Musset B, Limberg SH, Renigunta V, Sus R, Dalpke AH, Heeg KM, Robaye B, Hanley PJ. "Host tissue damage" signal ATP promotes non-directional migration and negatively regulates toll-like receptor signaling in human monocytes. J Biol Chem. 2005 Sep 16;280(37):32459-67. doi: 10.1074/jbc.M505301200. Epub 2005 Jul 19. PMID: 16030017.

40. Wegiel B, Larsen R, Gallo D, Chin BY, Harris C, Mannam P, Kaczmarek E, Lee PJ, Zuckerbraun BS, Flavell R, Soares MP, Otterbein LE. Macrophages sense and kill bacteria through carbon monoxide-dependent inflammasome activation. J Clin Invest. 2014 Nov;124(11):4926-40. doi: 10.1172/JCI72853. Epub 2014 Oct 8. PMID: 25295542; PMCID: PMC4347244.

41. Shiloh MU, Manzanillo P, Cox JS. Mycobacterium tuberculosis senses host-derived carbon monoxide during macrophage infection. Cell Host Microbe. 2008 May 15;3(5):323-30. doi: 10.1016/j.chom.2008.03.007. PMID: 18474359; PMCID: PMC2873178.

42. Collins A, Marciano D, Graviss E, Shiloh M. Role of Heme Oxygenase in the immune response to Mycobacterium tuberculosis in humans. J Immunol. 2013;190:125.

43. Soares MP, Marguti I, Cunha A, Larsen R. Immunoregulatory effects of HO-1: how does it work? Curr Opin Pharmacol. 2009 Aug;9(4):482-9. doi: 10.1016/j.coph.2009.05.008. Epub 2009 Jul 6. PMID: 19586801.

44. Arnoult D, Soares F, Tattoli I, Girardin SE. Mitochondria in innate immunity. EMBO Rep. 2011 Sep 1;12(9):901-10. doi: 10.1038/embor.2011.157. PMID: 21799518; PMCID: PMC3166463.

45. Ries M, Schuster P, Thomann S, Donhauser N, Vollmer J, Schmidt B. Identification of novel oligonucleotides from mitochondrial DNA that spontaneously induce plasmacytoid dendritic cell activation. J Leukoc Biol. 2013 Jul;94(1):123-35. doi: 10.1189/jlb.0612278. Epub 2013 Apr 22. PMID: 23610148.

46. Nathan C. Points of control in inflammation. Nature. 2002 Dec 19-26;420(6917):846-52. doi: 10.1038/nature01320. PMID: 12490957.

47. Molad Y, Pokroy-Shapira E, Carmon V. CpG-oligodeoxynucleotide-induced TLR9 activation regulates macrophage TREM-1 expression and shedding. Innate Immun. 2013 Dec;19(6):623-30. doi: 10.1177/1753425913476970. Epub 2013 Mar 8. PMID: 23475790.

48. Rodríguez-Flores E, Campuzano J, Aguilar D, Hernández-Pando R, Espitia C. The response of the fibrinolytic system to mycobacteria infection. Tuberculosis (Edinb). 2012 Nov;92(6):497-504. doi: 10.1016/j.tube.2012.07.002. Epub 2012 Aug 11. PMID: 22885283.

49. Radha KS, Sugiki M, Harish Kumar M, Omura S, Maruyama M. Post-transcriptional regulation of plasminogen activator inhibitor-1 by intracellular iron in cultured human lung fibroblasts--interaction of an 81-kDa nuclear protein with the 3'-UTR. J Thromb Haemost. 2005 May;3(5):1001-8. doi: 10.1111/j.1538-7836.2005.01272.x. PMID: 15869597.

50. González-Cortés C, Diez-Tascón C, Guerra-Laso JM, González-Cocaño MC, Rivero-Lezcano OM. Non-chemotactic influence of CXCL7 on human phagocytes. Modulation of antimicrobial activity against L. pneumophila. Immunobiology. 2012 Apr;217(4):394-401. doi: 10.1016/j.imbio.2011.10.015. Epub 2011 Nov 3. PMID: 22101183.

51. Goldbach-Mansky R. Immunology in clinic review series; focus on autoinflammatory diseases: update on monogenic autoinflammatory diseases: the role of interleukin (IL)-1 and an emerging role for cytokines beyond IL-1. Clin Exp Immunol. 2012 Mar;167(3):391-404. doi: 10.1111/j.1365-2249.2011.04533.x. PMID: 22288582; PMCID: PMC3374271.

How to cite this article: Cappelli G, Giovannini D, Basso A, Serafino A, Andreola F, Colizzi V, Mariani F. A New CpG ODN Induces a Fine-Tuning of Innate Response Resulting in *Mycobacterium tuberculosis* Containment. J Biomed Res Environ Sci. 2022 July 30; 3(7): 802-818. doi: 10.37871/jbres1517, Article ID: JBRES1517, Available at: https://www.jelsciences.com/articles/jbres1517.pdf